Mammea E/BB, an Isoprenylated Dihydroxycoumarin Protonophore That Potently Uncouples Mitochondrial Electron Transport, Disrupts Hypoxic Signaling in Tumor Cells

Lin Du,[†] Fakhri Mahdi,[†] Mika B. Jekabsons,[‡] Dale G. Nagle,*[,†,§] and Yu-Dong Zhou*[,†]

Department of Pharmacognosy and Research Institute of Pharmaceutical Sciences, School of Pharmacy, University of Mississippi, University, Mississippi 38677, United States, and Department of Biology, University of Mississippi, University, Mississippi 38677, United States

Received July 22, 2010

The mammea-type coumarin mammea E/BB (**1**) was found to inhibit both hypoxia-induced and iron chelator-induced hypoxia-inducible factor-1 (HIF-1) activation in human breast tumor T47D cells with IC_{50} values of 0.96 and 0.89 μM, respectively. Compound **1** suppressed the hypoxic induction of secreted VEGF protein (T47D cells) and inhibited cell viability/proliferation in four human tumor cell lines. Compound **1** (at 5 and 20 μM) inhibited human breast tumor MDA-MB-231 cell migration. While the mechanisms that underlie their biological activities have remained unknown, prenylated mammea coumarins have been shown to be cytotoxic to human tumor cells, suppress tumor growth in animal models, and display a wide variety of antimicrobial effects. Mechanistic studies revealed that **1** appears to exert an assemblage of cellular effects by functioning as an anionic protonophore that potently uncouples mitochondrial electron transport and disrupts mitochondrial signaling in human tumor cell lines.

The mammea-type coumarins are a large family of isoprenylated 5,7-dihydroxycoumarin metabolites from *Mammea americana* L. (Guttiferae/Clusiaceae) and other species of *Mammea*, *Mesua*, and *Calophyllum*.[1] Mammea coumarins have been shown to possess a wide array of biological activities. These prenylated coumarins act as radical scavengers,[2] are cytotoxic to human tumor cells,[2−6] suppress tumor growth in animal models,[7] and exhibit anti-HIV,[8] antifungal,[9] and antibacterial[4,10] activities. Recent studies indicate that the inhibitory effects exerted by mammea-type coumarins on tumor cell viability are mediated through mechanisms that involve mitochondrial dysfunction-mediated apoptosis[7,11,12] and to a lesser degree necrotic cell death.[7] However, the biochemical mechanisms by which this class of prenylated coumarins exerts such a broad range of effects on both eukaryotic and prokaryotic cells have remained unexplained. In a search for small-molecule HIF-1 inhibitors from natural sources, a lipid extract of the plant *M. americana* was found to inhibit hypoxia (1% O_2)-induced HIF-1 activation by 89% at 5 μg/mL in a human prostate tumor PC-3 cell-based reporter assay. Bioassay-guided fractionation of the active extract resulted in the isolation of the previously reported mammea-type coumarin mammea E/BB (**1**).[1] At submicromolar concentrations, **1** inhibited hypoxia-induced HIF-1 activation in human breast tumor T47D cells. Mechanistic studies have now revealed that **1** uncouples oxidative phosphorylation by suppressing the ability of cells to maintain the proton gradient required to drive mitochondrial ATP synthesis. Compound **1** uncouples respiration in T47D cells with a relative potency similar to that of the commonly used mitochondrial uncoupler FCCP (carbonyl cyanide *p*-trifluoromethoxyphenylhydrazone).

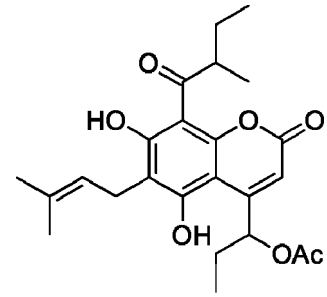

1

Results and Discussion

The transcription factor HIF-1 regulates the expression of many genes involved in key aspects of cancer biology and has emerged as an important tumor-selective molecular target for anticancer drug discovery.[15] Over 20000 lipid extracts from plants and marine organisms were evaluated in tumor cell-based reporter assays for HIF-1 inhibitory activities.[16] An active extract of the plant *M. americana* was subjected to bioassay-guided isolation to yield the compound mammea E/BB (**1**). The chemical structure of **1** was determined by comparison of its physicochemical properties and ^1H and ^{13}C NMR data with those previously published.[2,13,14]

Concentration−response studies were performed in human breast tumor T47D and prostate tumor PC-3 cells to determine the effects of **1** on HIF-1 activation using cell-based reporter assays. Compound **1** inhibited both hypoxia (1% O_2)-induced and iron chelator (10 μM 1,10-phenanthroline)-induced HIF-1 activation with comparable submicromolar IC_{50} values [0.96 μM (95% CI: 0.92−1.01 μM) and 0.89 μM (95% CI: 0.81−0.98 μM), respectively] in T47D cells (Figure 1A). The expression of luciferase from a control construct (pGL3-Control) was modestly suppressed (IC_{50} > 20 μM, data not shown). However, a loss of potency was observed in PC-3 cells [IC_{50} values: 2.0 μM (95% CI: 1.88−2.26 μM) for hypoxia-induced and 6.5 μM (95% CI: 5.18−8.10 μM) for iron chelator-induced HIF-1 activation, Figure 1B]. One possible explanation for this decrease in potency may lie in the different in vitro models that these two cell lines represent: T47D cells symbolize a highly inducible model for HIF-1 activation, and PC-3 cells a moderately inducible model (Nagle and Zhou, unpublished observations). As a result, cell lines that are representative of the moderate-induction model (PC-3) are less sensitive to HIF-1 inhibitors relative to those cell lines that are characterized by the highly inducible model (T47D).

One of the molecular mechanisms for hypoxia-stimulated tumor angiogenesis is the HIF-1-dependent induction of the potent angiogenic factor VEGF.[17] In T47D cells, hypoxic exposure (1%

* Joint corresponding authors. Tel: (662) 915-7026. Fax: (662) 915-6975. E-mail: dnagle@olemiss.edu (D.G.N.). Tel: (662) 915-7026. Fax: (662) 915-6975. E-mail: ydzhou@olemiss.edu (Y.-D.Z.).
[†] Department of Pharmacognosy.
[‡] Department of Biology.
[§] Research Institute of Pharmaceutical Sciences.

10.1021/np100501n
Published on Web 10/07/2010

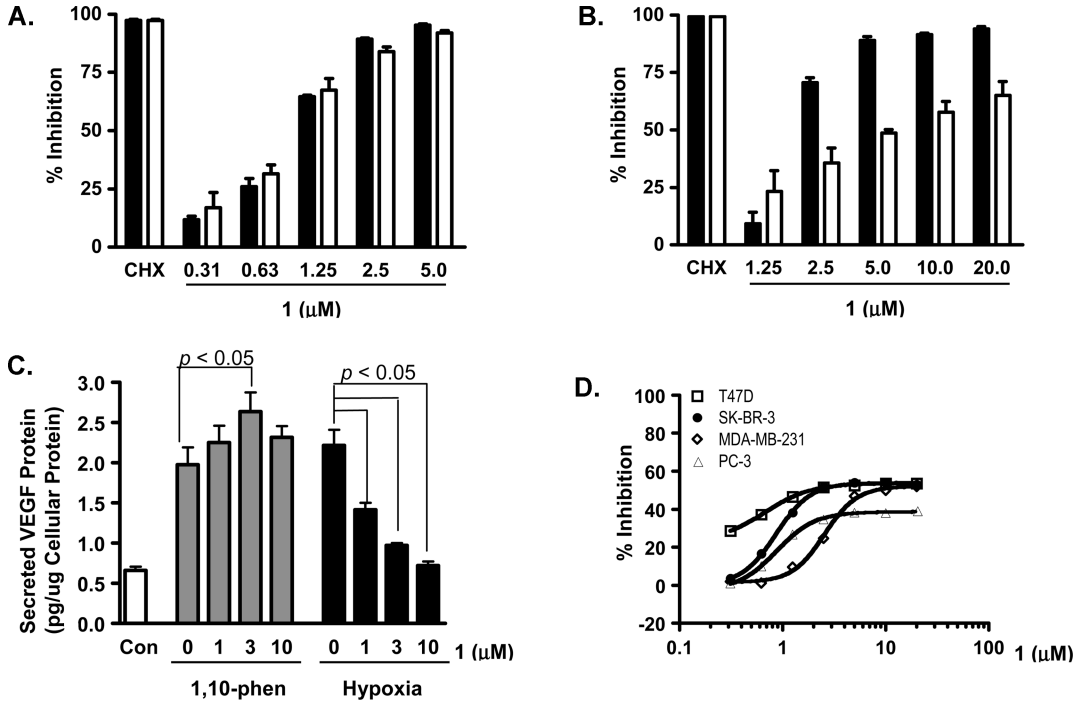

Figure 1. Mammea E/BB (**1**) inhibits HIF-1 activation and suppresses tumor cell proliferation/viability. (A) Compound **1** exhibited concentration-dependent inhibition of HIF-1 activation in a T47D cell-based reporter assay. The protein synthesis inhibitor cycloheximide (100 μM) was used as a positive control (CHX). The inducing conditions are (i) hypoxia (1% O_2, 16 h, solid bars) and (ii) chemical hypoxia (10 μM 1,10-phenanthroline, 16 h, open bars). Data shown are average + standard deviation from one experiment performed in triplicate (representative of two independent experiments). (B) Compound **1** inhibited HIF-1 activation in PC-3 cells. Experimental conditions and data presentation are the same as those described in (A). (C) Compound **1** inhibited hypoxic induction of secreted VEGF protein in T47D cells. T47D cells were exposed to 1,10-phenanthroline (10 μM, 16 h) or hypoxia (1% O_2, 16 h) in the presence of **1**. Levels of secreted VEGF protein in the conditioned media samples were determined by ELISA and normalized to the levels of cellular protein. Data shown are average + standard deviation ($n = 3$) from one experiment (representative of two independent experiments). Data were compared by one-way ANOVA followed by Bonferroni analysis. (D) Compound **1** suppressed the proliferation/viability of a panel of human tumor cell lines in a concentration-dependent manner. Human breast tumor T47D, SK-BR-3, and MDA-MB-231 and prostate tumor PC-3 cells were exposed to **1** at the specified concentrations for 48 h. Cell viability was determined by the sulforhodamine B method and presented as % inhibition of the untreated control. Data shown are averages from one experiment performed in triplicate, and the bars represent standard deviation.

O_2, 16 h) significantly increased the level of secreted VEGF protein (Figure 1C). Compound **1** (1, 3, and 10 μM) inhibited the hypoxic induction of secreted VEGF protein in a dose-dependent manner. However, **1** did not suppress the induction of secreted VEGF protein by the iron chelator 1,10-phenanthroline (Figure 1C). In general, mitochondrial respiratory chain inhibitors constitute one class of HIF-1 inhibitors that selectively suppresses HIF-1 activation induced by hypoxia, relative to their effects on chemical hypoxia (e.g., iron chelator)-induced HIF-1 activation.[18] Compound **1** is unique in the aspect that it inhibited 1,10-phenanthroline-induced HIF-1 activation in the cell-based reporter assay (Figures 1A and B) and enhanced 1,10-phenanthroline-induced production of secreted VEGF protein at the concentration of 3 μM (Figure 1C).

The effects of **1** on cell proliferation/viability were evaluated in a panel of human tumor cell lines (T47D, SK-BR-3, and MDA-MB-231 breast tumor and PC-3 prostate tumor cells). Compound **1** exhibited concentration-dependent inhibition of the proliferation/viability of all four cell lines (Figure 1D). At the highest concentration tested (20 μM), **1** inhibited cell proliferation/viability by 54%, 53%, 52%, and 40% following 48 h of compound treatment in T47D, SK-BR-3, MDA-MB-231, and PC-3 cells, respectively. The inhibitory effects appear to plateau at ~50% inhibition in T47D, SK-BR-3, and MDA-MB-231 cells and ~40% inhibition in PC-3 cells at the range of concentrations tested (0.31 to 20 μM). Short-term exposure produced a less pronounced inhibition of cell proliferation/viability (<30% inhibition after 16 h incubation under hypoxic conditions at concentrations up to 20 μM).

The metastasis of tumor cells to secondary sites is a major contributor to the relapse of cancer. To assess the effect of **1** on tumor cell migration, a metastatic human breast tumor MDA-MB-231 cell-based wound-healing assay was employed as an in vitro model. Following the generation of a scratch wound on a layer of confluent MDA-MB-231 cells, the surrounding cells migrated into the damaged area and healed the "wound" over a period of time (Figure 2A, control). Compound **1** (5 and 20 μM) suppressed the migration of MDA-MB-231 cells under both normoxic (95% air: 5% CO_2, 22 h) and hypoxic conditions (1% O_2:94% N_2:5% CO_2, 22 h) (Figure 2A). Under experimental conditions, **1** exerted modest inhibition on the viability of MDA-MB-231 cells (~25% inhibition at 20 μM, Figure 2B). Therefore, **1** suppressed tumor cell migration, and this was not a direct consequence of cytotoxicity. It is likely that the target(s)/pathway(s) affected by **1** regulates both cell migration and viability.

The *M. longifolia* farnesylated coumarin surangin B has been shown to exert pronounced antifungal activity via the disruption of mitochondrial electron transport by noncompetitively inhibiting complex II and by binding to the Qi site of complex III.[9,19] At extremely high micromolar to millimolar concentrations, certain simple coumarins stimulated mitochondrial respiration by uncoupling oxidative phosphorylation.[20−22] Recently, the mitochondrial uncoupler FCCP (carbonyl cyanide *p*-trifluoromethoxyphenylhydrazone) was reported to inhibit the stabilization of HIF-1α protein in rat carotid body glomus cells[23] and to decrease HIF-1 activity in PC-3 and DU-145 prostate cancer cells.[24] The compound FCCP

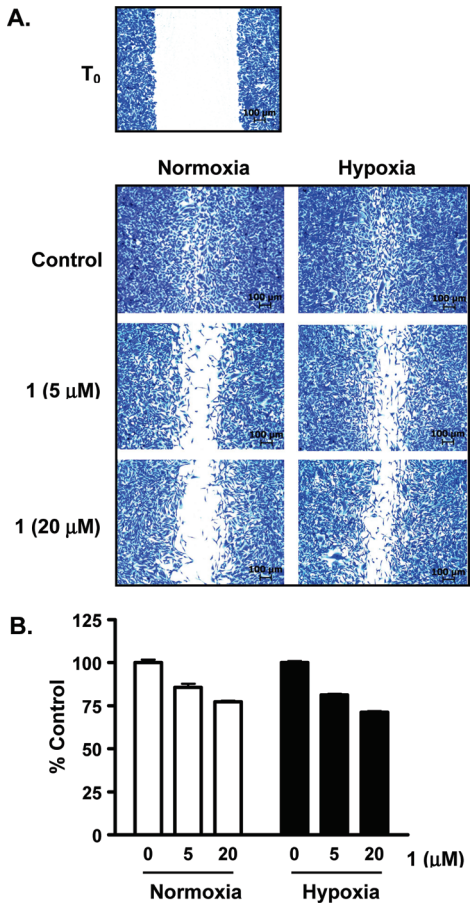

Figure 2. Mammea E/BB (**1**) suppresses the migration of MDA-MB-231 cells. (A) Compound **1** inhibited MDA-MB-231 tumor cell migration in a wound-healing assay. Wounds were created on a layer of confluent MDA-MB-231 cells by scratching with pipet tips (T_0). Compound **1** was added at the specified concentrations, and the incubation continued for 22 h, under normoxic (95% air) and hypoxic (1% O_2) conditions. The cells were fixed, stained, and imaged. Scale bars (100 μm) are included in each panel. (B) Compound **1** exhibited partial inhibition of MDA-MB-231 cell proliferation/viability under conditions used in the wound-healing assay. Cell viability (determined by the sulforhodamine B method) was presented as % control of the untreated cells under normoxic or hypoxic conditions, as appropriate. Data shown are average + standard deviation from one experiment performed in triplicate.

functions as a lipophilic cationic proton translocator that freely carries dissociable protons across membranes and dissipates the proton gradient. This process removes the proton gradient required to drive ATP synthesis. To test the hypothesis that **1** may inhibit hypoxic HIF-1 activation by functioning as an anionic proton translocator (mitochondrial uncoupler), we first examined the effect of **1** on cellular respiration. In a T47D cell-based respiration assay,[25] **1** exhibited biphasic effects on cellular oxygen consumption. At lower concentrations, **1** enhanced the rate of oxygen consumption (e.g., 30% increase at 1 μM) in comparison to the control (Figure 3A), consistent with the actions of a protonophore. At higher concentrations, **1** suppressed oxygen consumption (e.g., 50% decrease at 10 μM, Figure 3A). Similar biphasic concentration-dependent effects on cellular respiration were observed in the presence of the commonly used mitochondrial uncoupler FCCP (Figure 3A). To determine if **1** stimulates cellular respiration by uncoupling or by enhancing cellular ATP consumption, the effect of this compound on cellular respiration was measured in the presence of oligomycin, an inhibitor of F_0F_1ATPase. The inhibition of F_0F_1ATPase increases the proton gradient across the mitochondrial inner membrane, which then slows mitochondrial electron

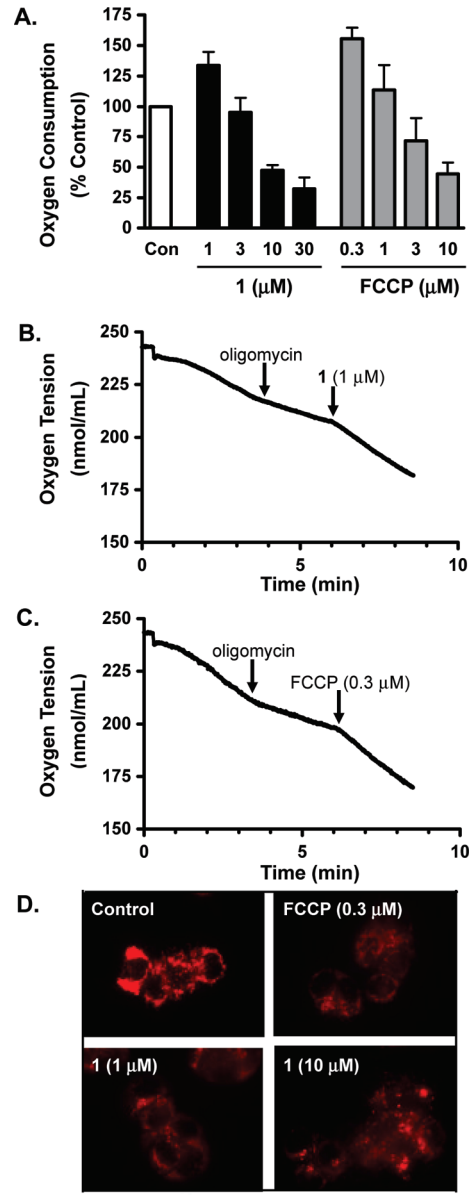

Figure 3. Mammea E/BB (**1**) uncouples mitochondrial respiration. (A) Compound **1** exhibited a concentration-dependent biphasic effect on cellular oxygen consumption in T47D cells. The commonly used uncoupler FCCP was included as a positive control. Data shown are average + standard deviation for **1** ($n = 3$) and average + deviation from average for FCCP ($n = 2$). (B) Compound **1** overcame oligomycin (1 μM)-inhibited T47D cellular respiration. (C) The uncoupler FCCP reinitiated respiration of oligomycin-treated T47D cells. (D) Compound **1** dissipated mitochondrial membrane potential. T47D cells were preincubated with the membrane potential-dependent dye $TMRM^+$, exposed to **1** and FCCP for 15 min, and imaged under an Axiovert 200 M epifluorescent microscope. Images shown are representative of each condition.

transport (reflected by the decreased rate of oxygen consumption, known as state 4 respiration, Figures 3B and C). Similar to that observed with uncouplers such as FCCP (Figure 3C), **1** stimulated state 4 respiration in T47D cells (Figure 3B), further supporting its possible action as a protonophore. To exclude the possibility that **1** increases state 4 respiration by stimulating mitochondrial substrate oxidation, in situ mitochondrial membrane potential was assessed with the fluorescent cationic dye tetramethyl rhodamine methyl ester (TMRM). The accumulation of TMRM in the mitochondrial matrix varies according to the magnitude of the

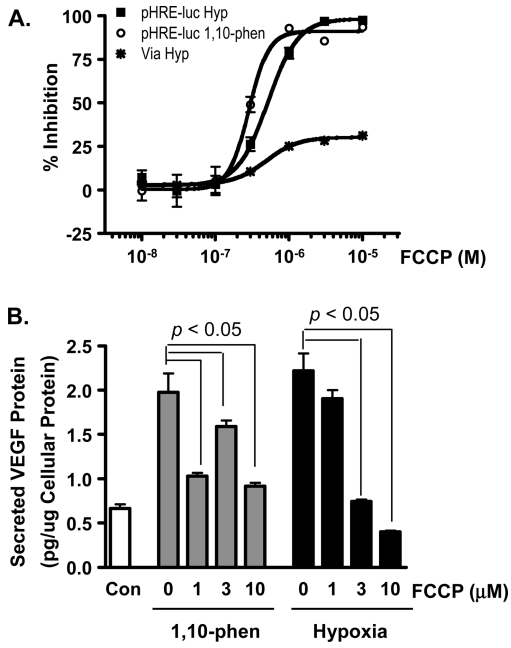

Figure 4. FCCP inhibits HIF-1 activation. (A) Concentration−response results of FCCP on HIF-1 activation induced by hypoxia (1% O_2, 16 h, pHRE-luc Hyp) and by iron chelator (10 μM 1,10-phenanthroline, 16 h, pHRE-luc 1,10-phen), and on T47D cell viability (1% O_2, 16 h, Via Hyp). Data shown are average ± standard deviation from one experiment performed in triplicate. (B) FCCP suppressed the induction of secreted VEGF protein by 1,10-phenanthroline and hypoxia in T47D cells. Experimental conditions and data presentation are the same as those described in Figure 1C.

mitochondrial membrane potential. The FCCP decreases mitochondrial inner membrane potential and results in diffused and faint TMRM staining (Figure 3D, FCCP). Compound **1** reduced mitochondrial membrane potential just as observed in the presence of FCCP (Figure 3D, **1** and FCCP). Thus, it is most likely that **1** acts as an uncoupler of oxidative phosphorylation at low micromolar concentrations and, in this way, may disrupt mitochondria-mediated HIF signaling.

To compare the effect of FCCP on HIF-1 activation with the effect observed in the presence of **1**, a concentration−response study was performed in a T47D cell-based reporter assay (Figure 4A). Treatment with FCCP inhibited hypoxia-induced HIF-1 activation with an IC_{50} value of 0.51 μM (95% CI: 0.46−0.57 μM) and 1,10-phenanthroline-induced HIF-1 activation with an IC_{50} value of 0.31 μM (95% CI: 0.27−0.37 μM). Under hypoxic conditions (1% O_2, 16 h), FCCP exhibited modest inhibition of T47D cell proliferation/viability (plateau at 25%, Figure 4A). In T47D cells, FCCP suppressed the induction of secreted VEGF protein by hypoxia in a concentration-dependent manner (Figure 4B). FCCP exhibited a less pronounced inhibitory effect on 1,10-phenanthroline-induced production of secreted VEGF protein at 3 μM than those observed at either 1 or 10 μM (Figure 4B). It has yet to be explained why FCCP and **1** each exerts atypical concentration-dependent effects on 1,10-phenanthroline-induced secreted VEGF protein production. However, the present studies do confirm the results obtained in an early human prostate tumor DU145 and PC-3 cell-based investigation that revealed FCCP (10 μM) inhibits HIF-1 activation.[24]

The previously reported farnesylated coumarin surangin[9,19] inhibited mitochondrial electron transport and, thereby, blocked cellular respiration. In contrast to the reported activity of surangin, **1** increased cellular respiration at lower concentrations as the cells respond in a compensatory manner to the decrease in mitochondrial proton gradient. Dissipation of the mitochondrial proton gradient eventually shuts down the electron transport chain. At elevated concentrations, **1** may also inhibit cellular respiration by directly suppressing the electron transport chain. This concentration-dependent effect exerted by **1** on cellular respiration is similar to that observed with FCCP, a commonly used uncoupler. In sharp contrast to the extremely weak mitochondrial uncoupling effects of simple substituted coumarins,[20−22] the highly lipophilic nature of **1** appears to facilitate mitochondrial membrane penetration and the subsequent translocation of protons from the intermembrane space to the matrix. This is likely because prenylation of the coumarin nucleus increases the lipophilic nature of the deprotonated anionic forms of these weakly acidic compounds, thereby facilitating the exchange of these proton translocators across lipophilic membranes. Mechanistic studies indicate that **1** affects cellular energetic and tumor cell viability by acting as an anionic protonophore that potently uncouples the mitochondrial proton gradient from ATP synthesis. The disruption of mitochondrial function by uncouplers such as FCCP and **1** may prevent the mitochondria-mediated induction of HIF-1α protein and the subsequent activation of HIF-1.

Experimental Section

Plant Material. *Mammea americana* stem bark was collected in Dominica (August 1992). The plant material was identified by Dr. Kendall Lee (New York Botanical Gardens, Bronx, NY). The NCI Open Repository number N071413 was assigned to the sample. A voucher specimen was deposited at the Smithsonian Institution National Museum of Natural History, Washington, DC.

Isolation of Mammea E/BB (1). Dried plant material was extracted with CH_2Cl_2−MeOH (1:1), residual solvents were removed under vacuum, and the extract (N071413) was stored at −20 °C in the NCI repository at the Frederick Cancer Research and Development Center (Frederick, Maryland). The organic extract (4.1 g) was subjected to Sephadex LH-20 column chromatography, using $CHCl_3$ with MeOH (1:1) as the mobile phase, to afford nine fractions. The third fraction (1.60 g) was further separated into six subfractions by C_{18} VLC column chromatography (eluted with step gradients of 10% to 100% MeOH in H_2O). The fourth subfraction (1.08 g, eluted with 80% MeOH in H_2O) was subjected to a Sephadex LH-20 column eluted with hexanes−CH_2Cl_2−MeOH (2:1:1). The fifth subfraction from the Sephadex LH-20 column (462 mg) was further separated by reversed-phase HPLC (Luna 5 μm, ODS-3, 100 Å, 250 × 10.00 mm, isocratic 85% CH_3OH in 0.1% TFA, 4.0 mL min^{-1}) to produce **1** (22.0 mg, 0.5% yield). The structure of **1** was confirmed by NMR analysis. The ^1H (400 MHz) and ^{13}C (100 MHz) NMR spectra were recorded in $CDCl_3$ on a Bruker DRX 400 NMR spectrometer. The NMR spectra were recorded using residual solvent peaks (δ 7.27 for ^1H and δ 77.0 for ^{13}C) used as internal references. The spectroscopic and physical characteristics of **1** were in agreement with those previously reported for mammea E/BB.[2,13,14] Compound **1** was determined to be >98% pure by HPLC.

Cell-Based Reporter and Proliferation/Viability Assays. Human breast tumor T47D, SK-BR-3, and MDA-MB-231 and prostate tumor PC-3 cells were purchased from ATCC and maintained in DMEM/F12 medium with L-glutamine (Mediatech), supplemented with fetal bovine serum [FBS, 10% (v/v), Hyclone] and a mixture of penicillin (50 units mL^{-1}) and streptomycin (50 μg mL^{-1}) (Lonza).

The cell-based reporter assay was performed as described with the pHRE3-TK-Luc construct to monitor HIF-1 activity.[16] For the cell proliferation/viability assay, exponentially grown cells were plated at a density of 30 000 cells per well into 96-well plates in a volume of 100 μL of culture media, and the plates were incubated at 37 °C overnight. Test compounds were added at the specified concentrations in a volume of 100 μL of serum-free media with penicillin and streptomycin. The incubation continued for another 48 h, and cell viability was determined by the sulforhodamine B method.[25] Data are presented as % inhibition calculated using the formula

$$\%\ \text{inhibition} = [1 - (OD_{treated}/OD_{control})] \times 100$$

ELISA Assay for Secreted VEGF Protein. The procedures were the same as previously described.[16] The levels of secreted VEGF protein in the T47D cell-conditioned media samples were determined by ELISA and normalized to the amount of cellular proteins quantified using a micro BCA assay kit (Pierce).

MDA-MB-231 Cell-Based Wound-Healing Assay. The plating of MDA-MB-231 cells, wound generation, compound treatment, staining, and imaging were the same as previously reported.[25]

Cellular Respiration Assay. An Oxytherm Clarke-type electrode system (Hansatech) was used to monitor oxygen consumption in T47D cells. Experimental procedures for the T47D cell-based respiration study were the same as previously described.[25] The level of oxygen consumption in the presence of compound was presented as % control using the formula

$$\%\ \text{control} = 100 \times (\text{oxygen consumption rate})_{\text{compound}} / (\text{oxygen consumption rate})_{\text{control}}$$

For the mechanistic studies, oligomycin was added to T47D cells at the final concentration of 1 μM. Compound **1** or the standard uncoupler FCCP (as a positive control, Sigma) was added at the specified concentrations to resume respiration suppressed by oligomycin.

Mitochondrial Membrane Potential Assay. T47D cells were plated at a density of 100000 cells per well into a two-well Lab-Tek II chambered coverglass (Nunc). After the cells attach to the coverglass (overnight), the conditioned media were replaced with a buffer that contains 20 mM TES, pH 7.3, 150 mM NaCl, 5 mM KCl, 1.3 mM $CaCl_2$, 1.3 mM $MgCl_2$, 5 mM glucose, 1.2 mM Na_2SO_4, 0.4 mM KH_2PO_4, 0.3% (w/v) BSA, and 2 nM TMRM (Molecular Probe). The cells were incubated with the membrane potential-dependent dye $TMRM^+$ at 37 °C for 1 h and 15 min. Test compounds were added and the incubation continued for another 15 min. Live cell imaging was performed with an Axiovert 200M epifluorescence microscope (Zeiss).

Statistical Analysis. Data were compared using one-way ANOVA followed by Bonfferoni post hoc analyses (GraphPad Prism 4). Differences were considered significant when $p < 0.05$.

Acknowledgment. The authors thank the Natural Products Branch Repository Program at the National Cancer Institute for providing marine extracts from the NCI Open Repository used in these studies, D. J. Newman and E. C. Brown (NCI, Frederick, MD) for assistance with sample logistics and collection information, and S. L. McKnight (University of Texas Southwestern Medical Center at Dallas) for providing the pTK-HRE3-luc construct. Funding was provided in part by the NIH/NCI grant CA98787 (D.G.N./Y.D.Z.) and NOAA/NIUST grant NA16RU1496. This investigation was conducted in a facility constructed with Research Facilities Improvement Grant C06 RR-14503-01 from the NIH.

References and Notes

(1) Yang, H.; Jiang, B.; Reynertson, K. A.; Basile, M. J.; Kennelly, E. J. *J. Agric. Food Chem.* **2006**, *54*, 4114–4120.
(2) Yang, H.; Protiva, P.; Gil, R. R.; Jiang, B.; Baggett, S.; Basile, M. J.; Reynertson, K. A.; Weinstein, I. B.; Kennelly, E. J. *Planta Med.* **2005**, *71*, 852–860.
(3) Lee, K. H.; Chai, H. B.; Tamez, P. A.; Pezzuto, J. M.; Cordell, G. A.; Win, K. K.; Tin-Wa, M. *Phytochemistry* **2003**, *64*, 535–541.
(4) Ouahouo, B. M. W.; Azebaze, A. G. B.; Meyer, M.; Bodo, B.; Fomum, Z. T.; Nkengfack, A. E. *Ann. Trop. Med. Parasitol.* **2004**, *98*, 733–739.
(5) Reyes-Chilpa, R.; Estrada-Muniz, E.; Apan, T. R.; Amekraz, B.; Aumelas, A.; Jankowski, C. K.; Vazquez-Torres, M. *Life Sci.* **2004**, *75*, 1635–1647.
(6) Lopez-Perez, J. L.; Olmedo, D. A.; Del Olmo, E.; Vasquez, Y.; Solis, P. N.; Gupta, M. P.; San Feliciano, A. *J. Nat. Prod.* **2005**, *68*, 369–373.
(7) Ruiz-Marcial, C.; Chilpa, R. R.; Estrada, E.; Reyes-Esparza, J.; Farina, G. G.; Rodríguez-Fragoso, L. *J. Pharm. Pharmacol.* **2007**, *59*, 719–725.
(8) Bedoya, L. M.; Beltran, M.; Sancho, R.; Olmedo, D. A.; Sanchez-Palomino, S.; del Olmo, E.; Lopez-Perez, J. L.; Munoz, E.; San Feliciano, A.; Alcami, J. *Bioorg. Med. Chem. Lett.* **2005**, *15*, 4447–4450.
(9) Deng, Y.; Nicholson, R. A. *Planta Med.* **2005**, *71*, 364–365.
(10) Verotta, L.; Lovaglio, E.; Vidari, G.; Finzi, P. V.; Neri, M. G.; Raimondi, A.; Parapini, S.; Taramelli, D.; Riva, A.; Bombardelli, E. *Phytochemistry* **2004**, *65*, 2867–2879.
(11) Alvarez-Delgado, C.; Reyes-Chilpa, R.; Estrada-Muniz, E.; Mendoza-Rodríguez, C. A.; Quintero-Ruiz, A.; Solano, J.; Cerbon, M. A. *J. Biochem. Mol. Toxicol.* **2009**, *23*, 263–272.
(12) Ito, C.; Murata, T.; Itoigawa, M.; Nakao, K.; Kaneda, N.; Furukawa, H. *J. Pharm. Pharmacol.* **2006**, *58*, 975–980.
(13) Laphookhieo, S.; Maneerat, W.; Kiattansakul, R. *Can. J. Chem.* **2006**, *84*, 1546–1549.
(14) Crombie, L.; Jones, R. C. F.; Palmer, C. J. *J. Chem. Soc., Perkin Trans. 1* **1987**, 317–331.
(15) Semenza, G. L. *Oncogene* **2010**, *29*, 625–634.
(16) Hodges, T. W.; Hossain, C. F.; Kim, Y.-P.; Zhou, Y.-D.; Nagle, D. G. *J. Nat. Prod.* **2004**, *67*, 767–771.
(17) Ferrara, N.; Mass, R. D.; Campa, C.; Kim, R. *Annu. Rev. Med.* **2007**, *58*, 491–504.
(18) Nagle, D. G.; Zhou, Y.-D. *Phytochem. Rev.* **2009**, *8*, 415–429.
(19) Deng, Y.; Nicholson, R. A. *Pestic. Biochem. Physiol.* **2005**, *81*, 39–50.
(20) Pai, M. R.; Bai, N. J.; Venkitasubramanian, T. A.; Murthy, V. V. *Environ. Physiol. Biochem.* **1975**, *5*, 184–188.
(21) Pai, M. R.; Bai, N. J.; Venkitasubramanian, T. A.; Murthy, V. V. *Toxicology* **1975**, *4*, 297–303.
(22) Papa, S.; Lofrumento, N. E.; Paradies, G.; Quagliariello, E. *Biochim. Biophys. Acta* **1969**, *180*, 35–44.
(23) Baby, S. M.; Roy, A.; Lahiri, S. *Histochem. Cell Biol.* **2005**, *124*, 69–76.
(24) Thomas, R.; Kim, M. H. *Mol. Cell. Biochem.* **2007**, *296*, 35–44.
(25) Liu, Y.; Veena, C. K.; Morgan, J. B.; Mohammed, K. A.; Jekabsons, M. B.; Nagle, D. G.; Zhou, Y.-D. *J. Biol. Chem.* **2009**, *284*, 5859–5868.
(26) Klimova, T.; Chandel, N. S. *Cell Death Differ.* **2008**, *15*, 660–666.

NP100501N